BOLLETTINO DI GEOFISICA TEORICA ED APPLICATA VOL. 39, N. 4, pp. 285-302; DECEMBER 1998

Stress field, deformations and displacements around a flat cavity in an elastic medium

M. CAPUTO [1] and R. CONSOLE [2]

[1] *Physics Department, University La Sapienza, Roma, Italy*
[2] *Istituto Nazionale di Geofisica, Roma, Italy*

(Received February 24, 1998; accepted October 15, 1998)

Abstract. The stress and displacement fields in an elastic medium containing a cavity limited by an ellipsoid of revolution are computed when the medium is subject to a generic shear parallel to the equatorial plane of the cavity, or to a tension or compression normal to the equator, when the surface of the cavity is subject to a normal stress, and the flattening of the cavity is assumed at 0.900, 0.990, 0.999. It is found that the maximum shear stress, at the points of maximum curvature of the cavity, for a flattening of 0.990, which is a possible value for the border of the irregular faults inside the crust of the Earth or for the dikes of magmatic chambers, may be 130 times the shear applied to the medium and the tilt may reach values of one minute of arc for a shear 10^{-5} the rigidity of the medium. These exceedingly large maximum shear stresses at the points of maximum curvature of the cavity could be reached in dikes of magmatic chambers when the migration of isothermal surfaces increases the temperature of the gases by a few degrees centigrade or when it causes a phase change with dilatation. The large maximum shear stresses at the border of the magmatic chamber are sufficient to cause the propagation of pre-existing fractures or the generation of new ones.

1. Introduction

In seismology it is often assumed that the geologic faults are geometrically described by ellipsoids of revolution with an almost unit flattening.

The cases when the elastic medium, where the ellipsoidal cavity is embedded, is subject to a shear parallel to the equator of the ellipsoid, or to a tension or compression normal to it, and the

Corresponding author: R. Console; Istituto Nazionale di Geofisica, Via di Vigna Murata 605, 00143 Roma Italy; tel. +39 06 518 604 17; fax +39 06 504 11 81; e-mail: console@ing750.ingrm.it

cavity is subject to normal tension or compression are of great interest in the geologic and volcanologic applications since they represent practical cases of magmatic chambers or faults.

The problem is of interest also to studies of Earth's deformations, which are often observed in underground cavities, because the cavity modifies the strain field in the vicinity, as pointed out by King and Bilham (1973), who also suggested that this effect could account for many of the inconsistencies in tidal tilt observations.

Harrison (1976) and Sato and Harrison (1990) estimated this effect and found that in fact relevant corrections are needed when the observations of strain are made in cavities where, for instance, the tilt on the surface of the cavity may have great variations from place to place. In some particular cases, as we shall see here, there are points where the tilt may vanish.

Of particular interest is the study of the stress field around the cavity because it governs the possible generation of successive fractures.

The problem was discussed by Neuber (1937, 1958) who gave a general theory to study the cases in which the body is subject to several types of forces and the surface of the cavity is free of stress. Eshelby (1957) solved the problem of the deformation of an ellipsoidal cavity in an infinite isotropic medium in which the strain becomes uniform at large distances from the cavity.

Keilis Borok (1959) applied the theory of Neuber (1937, 1958) to the limiting case when the cavity has unity flattening. Caputo (1990) extended the solution of Neuber to cases in which the ellipsoidal cavity is subject to normal tension or compression normal to its surface and when the deformation is governed by stress strain relations containing a memory mechanism.

In this note we shall apply the formulae of Caputo (1990) to compute the displacement field, the maximum shear stress field (*mss*) and its direction in cases when the medium and/or the cavity are subject to several types of forces. We find that there is a tubular region around the equator with a large stress concentration and that the concentration factor, in general, is inversely proportional to the maximum radius of curvature at the equator. Possible fractures in this region and their orientations are also discussed.

The variation of tilt from point to point on the surface of the cavity, when the medium is subject to shear, tension or compression, is also computed.

2. The cases discussed

In the following we make use of an ellipsoidal coordinate system u, v, w:

$$\begin{gathered} x = I \sinh u \cos v \\ y = I \cosh u \sin v \cos w \\ z = I \cosh u \sin v \sin w \\ I^2 = (x^2 + y^2)/\cosh^2 u + z^2/\sinh^2 u \end{gathered} \tag{1}$$

with a first fundamental form

$$\begin{gathered} ds^2 = h^2 (du^2 + dv^2) + h_w^2 dw^2; \\ h^2 = I^2 (\cosh^2 u - \sin^2 v);\ h_w = I \cosh u \sin v \end{gathered} \tag{2}$$

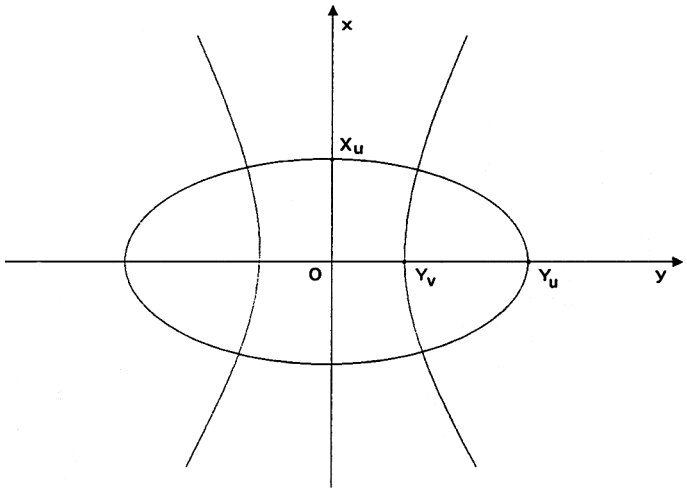

Fig. 1 - The geometry of the problem introduced in this study. The surfaces u = const. are ellipsoids of revolution with equation $x^2/I^2 \sinh^2 u + (y^2 + z^2)/I^2 \cosh u = 1$; the surfaces v = const. are hyperboloids of revolution with equation $-x^2/I^2 \cos v + (y^2 + z^2)/I^2 \sin v = 1$; the surfaces w = const. are planes through the x axis with equation $z = y \tan w$. The figure illustrates the section of these surfaces with the x, y plane. $OX_u = I \sinh u$, $OY_u = I \cosh u$, $OY_v = I \sin u$.

and assuming that the ellipsoidal cavity is defined by $u = u_o$ = const., with $u_o = 0.1$, $u_o = 0.01$, $u_o = 0.001$. Here I is a scaling factor, assumed as $I = 1/\cosh u_o$. Fig. 1 shows the geometry and orientation of the cavity in a rectangular coordinate system.

Since the solutions for cases in which the medium is subject to shear, tension or compression and the surface of the cavity is subject to a normal stress are linear, the problem of the computation of the strain and displacement fields, due to a linear combination of the two different types of stresses applied to the medium and normal forces applied to the surface of the cavity, is readily solved.

The corresponding *mss* and angles should obviously be computed combining the displacement, deformation or stress fields resulting from the applied forces linearly.

The formulae for the computation of the diagonal components σ_u, σ_v and σ_w, and of the non diagonal terms τ_{uv}, τ_{uw} and τ_{vw} of the stress tensor and the components U, V and W of the displacement when the medium is subject to a shear p_1 parallel to the x axis and the surface of the cavity is free of stress are given in the Appendix A. These formulae are reproduced to correct a few of Caputo misprints (1990).

The ellipsoidal cavities have symmetry of revolution around the x axis. The flattening f and the radius of curvature ρ of the ellipse at the intersection of the ellipsoids with the x,y plane, in the point of maximum curvature of the ellipse ($u = u_o$, $v = 90°$), are respectively

$$f = 1 - \tanh u_o \,, \qquad \rho = I \sinh^2 u_o / \cosh u_o .$$

For the cases considered here we have

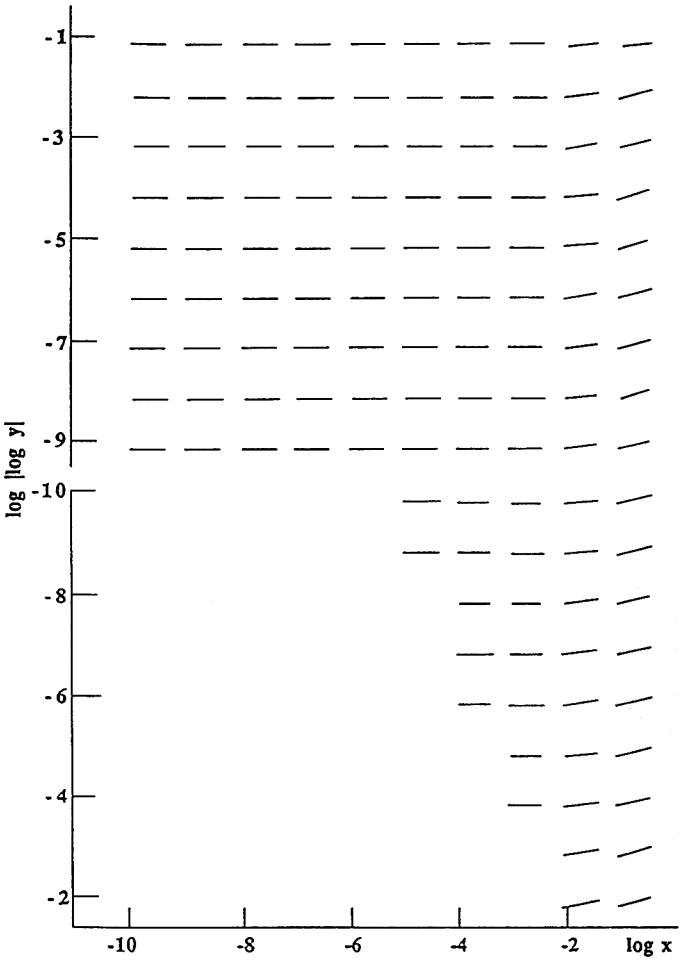

Fig. 2 - Displacement vectors in the first quadrant of the x, y section of the elastic medium containing the ellipsoidal cavity with unit semimajor axis along the y axis, $u_o = 0.01$ and $p_1 = \mu$, that is the medium is subject to a shear parallel to the x and y axes and nominally equal to the rigidity of the medium. The segments represent the displacement in arbitrary units.

$$\begin{array}{lll} u_o=0.1, & f=0.900, & \rho=9.98\ 10^{-3}\ I \\ u_o=0.01, & f=0.990, & \rho=1.00\ 10^{-3}\ I \\ u_o=0.001, & f=0.999, & \rho=1.00\ 10^{-3}\ I \end{array} \tag{3}$$

2.1. The case when a shear is applied to the medium

The results of the computations of the displacement field for $u_o = 0.01$, which of the three cases considered is the most significant, assuming first $p_1 = \mu$ (where μ is the rigidity of the medium) in rather large grids of the x, y plane in the neighbourhood of the point $x = z = 0$, $y = I$ are presented in Fig. 2; they are not indicative of particular features. Using the log |log y| as the

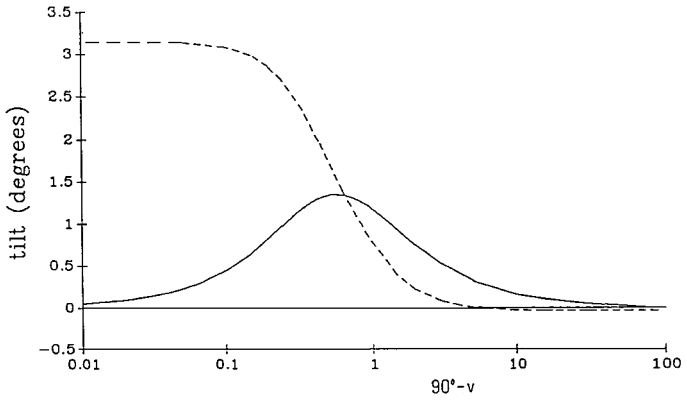

Fig. 3 - Tilt of the surface of the ellipsoidal cavity in the x, y plane ($u = u_o = 0.01$) versus v. The dashed line represents the tilt produced by a shear parallel to the x and y axes nominally equal to 10^{-3} times the rigidity of the medium. The solid line represents the tilt produced by a tension p_1 parallel to the x axis nominally equal to 10^{-3} times the rigidity of the medium.

parameter represented in the ordinates in this and in some similar figures which follow allows a magnification of the scale around the value $y = I$, where the most critical changes of both displacement and stress occur.

The displacements in the elastic medium subject to shear stress p_1 modifies the shape of the cavity, so that the stress could be estimated measuring the tilt at some points of its surface. On the section of the x, y plane, for the case $u_o = 0.01$, the tilt has a relative minimum in the point $v = 0$ (Fig. 3). Its value there, for $p_1 = \mu\ 10^{-3}$, is -0.037° . It increases with y, until it crosses zero at $v = 84.5°$ ($y = 0.995\ I$). Then it keeps increasing more and more rapidly until it reaches the absolute maximum of 3.15° at $y = I$.

The results of the computation of the *mss* for the case $u_o = 0.01$, also limited to the same region of the x, y plane, are shown in Fig. 4 where the directions of the planes of the *mss* are also given.

The values of *mss* resulting from the values of p_1 different to μ are obtained from the values of Fig. 4 by multiplying the values of Fig. 4 by the new value of p_1 in units of μ. Thus, *mss* is invariant with respect to p_1.

Concerning Fig. 4, it is seen that in a very limited region at the sides of the points of maximum curvature of the ellipse at the intersection of the ellipsoid with the x, y plane, there is a large gradient of the *mss*, resulting from a large gradient of the component τ_{uv} of the stress tensor, which reaches values of about thirty times larger than the applied shear stress.

In Figs. 5 and 6 we may see the *mss* in the plane $x = 0$. Along the equatorial line of the cavity $v = 90°$, $u = u_o$, for $0 < w < 90°$, there is a cylindrical region with a normal section with a diameter of $(4 \cdot 10^{-3})\ I$ where the *mss* reaches values larger than $10\ p_1$.

Assuming that p_1 is sufficiently small at the beginning and slowly increases, it will eventually reach a value sufficient to form a new fracture in this region of large stress concentration.

The orientation of the planes of the maximum *mss* in the limited region around the point

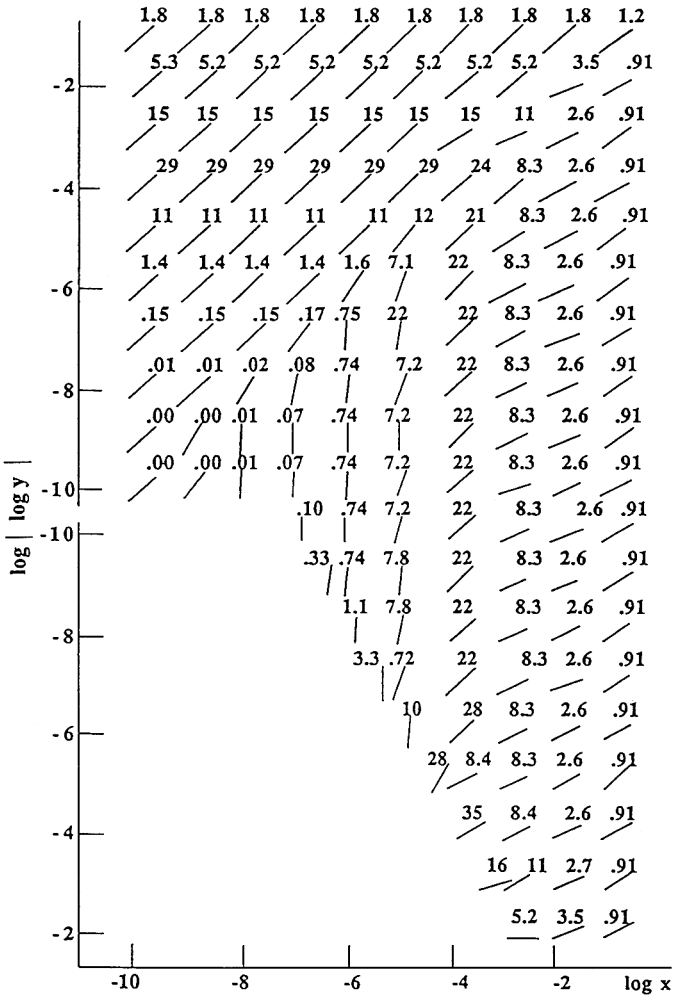

Fig. 4 - The maximum shear stress (*mss*) for the same values of the parameters and ellipsoidal section of Fig. 1. The numbers give the value of the *mss* in units of $p1$. Two principal directions are in the x, y plane, in each point one of them is given by the segment and the *mss* plane is at 45° angle with the x, y plane.

$x = z = 0$, $y = I$ are perpendicular to the x,y plane; their traces in this plane are parallel to the x and y axes respectively and indicate that new fractures may be generated with this orientation.

The formation of the new fracture will alter the *mss* field of Figs. 4, 5 and 6 and release part of it.

Neuber (1958) states that the maximum of the *mss*, in the case of an applied pure shear, occurs at the surface of the cavity at the point $x = 0$, $y = 0$, $z = I$ and is given by the formula

$$S = 4\, p_1\, \alpha/\pi\, (\alpha + 2) \sinh u_o \tag{4}$$

where $\alpha = 2\,(1 - 1/m)$ and $1/m$ is the Poisson ratio which is assumed here at 0.25.

S, for $u_o = 0.01$, is 55 p_1 and is shown in Figs. 5 and 6.

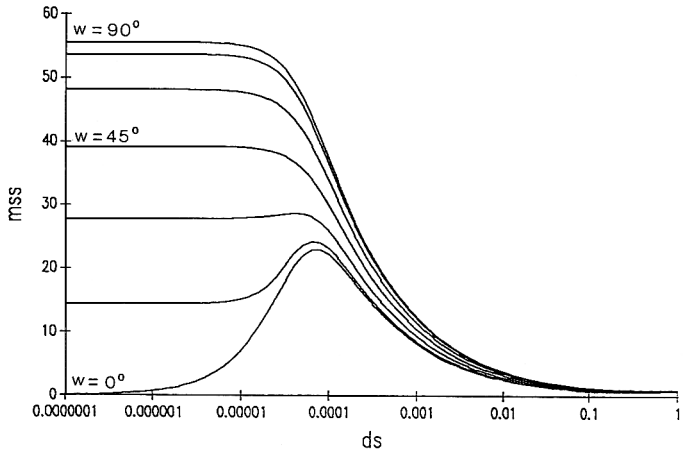

Fig. 5 - The values of the *mss* in the section $x = 0$ along the line $v = \mu/2$ for $\mu/2 > w > 0$ and $u_o = 0.01$. The ordinate shows the value of the *mss* in units of p, the abscissas is the distance from the surface of the ellipsoidal cavity in radial direction.

The planes of the *mss* in this point are at angles of 45° with the $y = 0$ plane and parallel to the z axis; the new fracture would most probably begin in that plane and propagate along the equator.

The region described above, when w approaches zero, approaching the point $x = y = 0$, $z = I$, becomes narrower while the value of *mss* approaches the value 55 p_1 given by (4).

In cases with $u_o = 0.1$ and $u_o = 0.001$ we have verified the existence of a similar cylindrical region of concentration of stress along the equator; the maximum *mss* of the region changes according to formula (7), it is 6.5 p_1 when $u_o = 0.1$ and 550 p_1 when $u_o = 0.001$.

For all values of u_o considered, the region always has the shape of a cylinder running along the equator of the cavity, reducing its diameter slightly when approaching the point $x = y = 0$, $z = I$ ($u = u_o$, $v = 90°$, $w = 0$) where it reaches the maximum concentration of *mss* given by (4).

For w decreasing along $v = 90°$, the *mss* decreases and for $w < 6°$ it is negligible. However, for $w < 6°$ the cylindrical region does not include the equator of the cavity, but runs parallel to it, and the maximum of the *mss* in it is always larger than 50% of the maximum *mss* in the cylindrical region given by (4).

For $w < 6°$ the maximum *mss* is reached at a distance of $I\,u_o^2$ from the equator and the diameter of the region there, is of the same order.

The *mss* in this cylindrical region, for $u_o < 0.1$ and for distances of the order of $I\,u_o^2$, falls at a rate $0.5\,S/\log d$ where S is given by formula (4) as function of u_o and d is the distance from the equator; at larger distances the rate is significantly and increasingly smaller.

Among the effects of p there is also a change of the shape of the cavity Σ; this in turn reduces its volume and causes a negative pressure on Σ; however the change in volume and the consequent pressure are negligible. The same cannot be said of the normal to Σ; to estimate it we consider a shear parallel to the x, y plane nominally equal to $10^{-3}\,\mu$ in the case Σ has a flattening

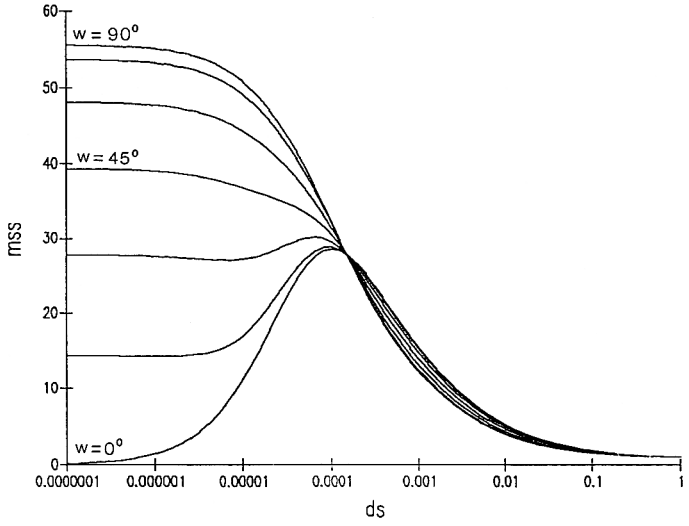

Fig. 6 - Values of the *mss* as in Figure 3 but here the distance from the plane $x = 0$ is in the abscissas.

of 0.99; at distances smaller than 0.017 I from the x,y plane this shear causes a tilt of Σ larger than one degree as shown in Fig. 3.

2.2. The case of tension and compression in the medium with normal forces applied to the surface of the cavity

In the case when the medium is subject to a tension or compression p normal to the equator of the cavity and this is subject to a normal tension or compression k the formulae are presented in Appendix B.

It is to be noted first, that when the cavity is spherical (Caputo, 1987) and the medium is subject to pure tension or compression, the *mss* occurs at the surface of the cavity. We shall see here, that by removing the spherical symmetry of the geometry of the cavity and the boundary conditions, the distribution of the *mss* changes and takes interesting forms.

In the case of this section, the stresses and displacements obviously have a revolution symmetry and it will be sufficient to compute them in the plane x, y.

In this case we will consider the cavity with $u_o = 0.01$ subject to a compression $k = -\mu$ ($k < 0$) normal to its surface and the medium subject to a tension $p = - k$ normal to its equatorial plane.

In Fig. 7 the displacement field caused by this set of forces is shown in the x, y plane and in the neighbourhood of the point $x = z = 0$, $y = I$.

As to the shape of the cavity, also in this case, the tension p in the medium produces modifications that can be observed through the tilt at the surface of the cavity. In the x, y plane, the tilt is null both in point $v = 0$ and in point $v = 90°$ (Fig. 3). For $u_o = 0.01$, the maximum is reached on the point Q at $v = 89.4°$ ($y = 0.99996\ I$), where its value is 1.3° for $p = \mu \cdot 10^{-3}$.

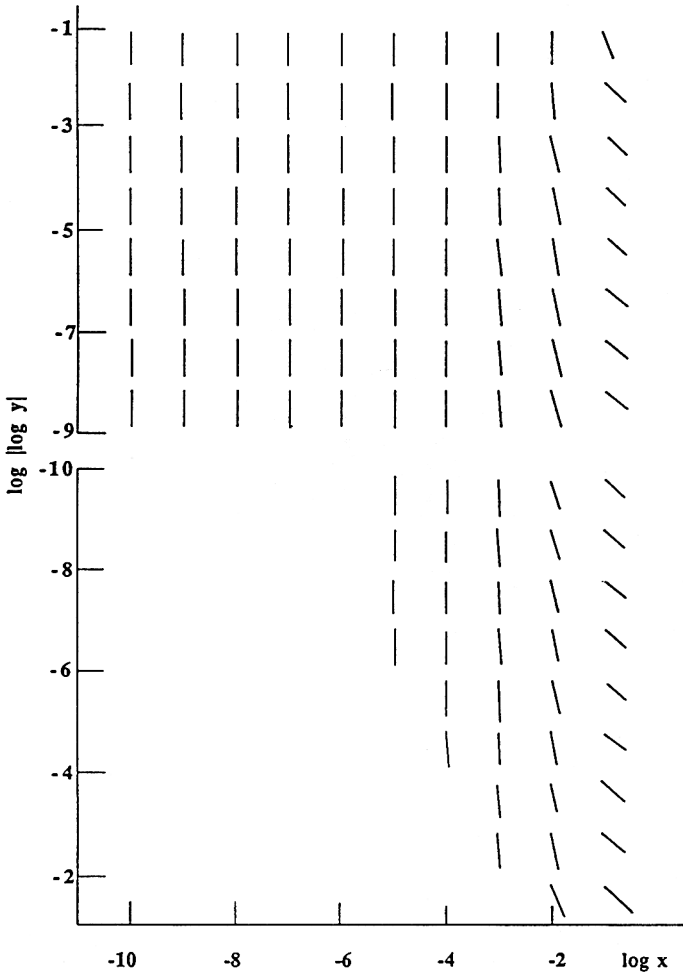

Fig. 7 - Displacements caused by a tension p, nominally equal to the rigidity of the medium and parallel to the x axis, and a pressure $k = -p$ applied to the surface of the ellipsoidal cavity with $u_o = 0.01$. The segments represent the displacement in arbitrary units. Due to the symmetry of revolution around the x axis the displacements are the same on all sections with planes through the x axis.

This implies that a tiltmeter in the top or bottom points of the cavity Σ would record no variation of the direction of the normal, while a tiltmeter located in Q would indicate a large change of this direction relative to the other points of Σ. The cavity Σ then functions as a magnifier and the best position to locate a tiltmeter to observe p, would be Q.

Fig. 8 shows the *mss* caused by the same forces and in the same region. It is seen that mss reaches its maximum value 128 p in the points of the circle $y^2 + z^2 = I^2$ of the plane $x = 0$.

Around the equatorial plane there is a cylindrical region which includes the equator of the cavity whose normal section has a radius of $I\, u_o/10$ where the *mss* is larger than 10 p.

The planes of *mss* in this region, in each point of the equator, are tangent to the equator and form an angle $\pi/4$ with the x axis. The values of the *mss* in this region are presented in Fig. 9.

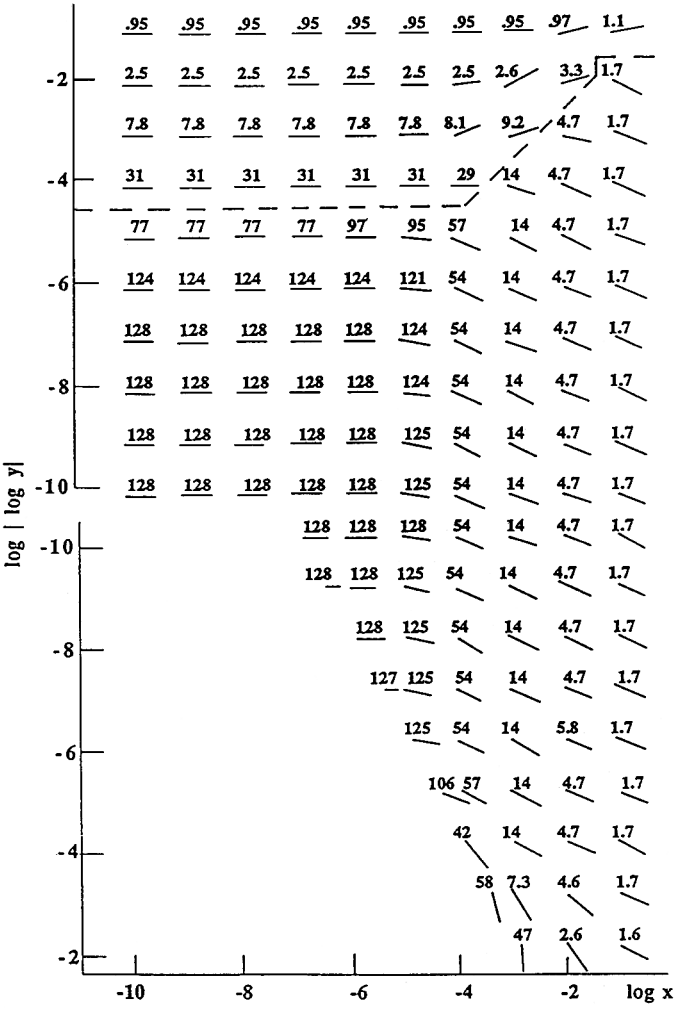

Fig. 8 - Values of the mss in section $x = 0$ for the same values as the parameters in Fig. 5. The numbers give the value of the *mss* in units of p. One of the principal directions is normal to the x, y plane, another is given by the segments; in those above the dotted line the direction of the segment and the normal to the x,y plane give the plane of the *mss* which is at $\pi/4$ angle with the x, y plane and at $\pi/2$ angle with the segment; in those below the dotted line, the segments and the principal direction normal to it in the x, y plane give the *mss* plane which is at $\pi/2$ angle with the x, y plane and at $\pi/4$ angle with the segment. Due to the symmetry of revolution around the x axis, the values and directions are the same on all sections with planes through the x axis.

The computation for the cases when $u_o = 0.1$ and $u_o = 0.001$ indicates that in the range $0.001 < u_o < 0.1$ the maximum *mss* is proportional to u_o and 13 p and 1280 p respectively for the extreme values.

Due to the symmetry of revolution, in the case of this paragraph, there is a cylindrical region around the equator with radius u_o for $u_o = 0.01$, radius 0.8 u_o for $u_o = 0.01$ and radius 0.008 u_o for $u_o = 0.001$, where the *mss* is larger than 0.1 p/u_o.

A fracture beginning at any point of weakness will therefore propagate along the equator of

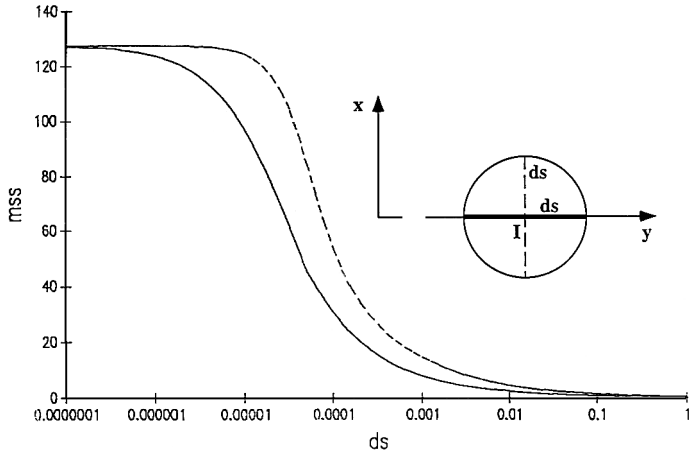

Fig. 9 - Values of the *mss* in section $z = 0$ as function of the distance from point $x = z = 0$, $y = I$ with $u_0 = 0.01$ and $p = -k = \mu$. The solid line gives the values of the *mss* as function of the distance from point $x = z = 0$, $y = I$ and along the y axis, the dashed line gives the values of the mss as function of the distance from the same point along the line $y = I$, $z = 0$.

the cavity while the dislocations will be at an angle of 45° with the equatorial plane and normal to the equator.

At the end of this process, along the equator, there will be a new fracture "en echelon" with the equator. The width of the fracture will obviously depend on the stress drop and the type of rock.

It is to be noted that when $p = \pm \mu$, $k = 0$ or $p = 0$, $k = \pm \mu$, the results will change in the signs, and the components of the stress tensor will be half the values obtained when $p = -k = \mu$.

The considerations in this section are of particular interest when studying the variation of pressure inside a sealed magmatic chamber due to a temperature induced volume change or to the formation of gases.

In fact, considering a dike of a magmatic chamber with a flattening of 0.99, assuming $p = 5$ bar we find that the *mss* reaches a value of 650 bar in the region of maximum curvature. This stress could be sufficient to cause new fractures and to extend the size of the dike.

Migration of isothermal surfaces may cause phase changes and possibly dilatations in the layers through which they go (Marechal, 1975). If the phase change occurs in magma sealed in a magmatic chamber, the dilatation would then cause pressure on the walls of the magmatic chamber.

The migration of the isothermal may also cause an increase of the pressure of the gases contained in the magma, which in turn would also cause an increase of the pressure on the walls of the magmatic chamber.

Finally, the migration of isothermal surfaces may just cause dilatations in the magmas and in the surrounding rocks without phase changes but with a different coefficient of thermal expansion of the magma and of the rocks which in turn would generate a pressure change on the wall of the magma chamber.

An example is in the Phlaegrean Fields in Italy where in the interval between 1970-1972 a change of 10°C (Palumbo, 1978) of the soil was recorded and in the interval between June 1970 - September 1972 a dilatation of 10^{-4} was accumulated (Caputo, 1979).

A thermal volume expansion coefficient of the magma and of the surrounding rocks of about $2 \cdot 10^{-5}$ °C^{-1} would cause the observed surface dilatation.

A difference in the thermal volume expansion coefficients, between the magma and the surrounding rocks, of about $3 \cdot 10^{-6}$ °C^{-1} would cause an increase of 5 bar in the pressure of the magma which would cause the supposed *mss* of 650 bar on the dikes of the magmatic chamber.

2.3. Effect of the rheology

As regards the rheology of the medium, we note that it plays an important role in the concentration of stress in cavities where the medium is subject to stress. In general, when the surface of the cavity is free of stress and the body is subject to tension (pressure) normal to the equator of the cavity, then the maximum shear stress at the equator of the cavity decreases (increases) with time (Caputo, 1990).

In the case of an ellipsoidal magmatic chamber imbedded in a crust free of stress, a pressure normal to the surface of the cavity generates the largest maximum shear stress at the equator and the stress decreases in time. However, if the pressure increases at a rate faster than the relaxation caused by the rheology, then the stress at the equator increases in time. If a pressure is acting in the medium normal to the surface of the cavity and is lower than the pressure acting on its surface, then the stress at the equator increases in time. These considerations are valid also for geologic faults containing gases or fluid at high pressure.

The discussion of the effects of the rheology on the stress field at the surface of the cavity may have a relevant impact on the stress corrosion theory, which may apply to the equator of the cavity itself. In this case, however, one may have contrasting effects. In fact, the increase of the radius of curvature ρ at the equator of the cavity causes a decrease of the local maximum shear stress but, it also favours the circulation of the fluid causing the corrosion. The decrease of the radius of curvature ρ at the equator increases the maximum shear stress but, on the other hand, it reduces the local circulation of fluid.

3. Conclusions

We have estimated the displacement and stress fields in a medium containing an ellipsoidal cavity Σ, with symmetry of revolution, in cases when the medium is subject to tension or compression normal to the equatorial plane of Σ or to a shear parallel to it, and assuming also that Σ is subject to a normal stress.

As already known, Σ may significantly alter both fields, especially when its flattening is large. However, the maximum shear stress and tilts in Σ, as function of the curvature at the equator of Σ where the curvature is maximum, has not been estimated. It is found here that, on the

surface of Σ both fields are extremely large at the points where the curvature of Σ is large.

When the flattening is of 0.99, a value which may occur in natural faults and underground cavities, in the region of maximum curvature, the maximum shear stress caused by a stress parallel to the equator of Σ, may be 130 times the applied shear stress. The tilt, for a shear 10^{-5} times the rigidity of the medium, which is a reasonable value, may be one minute of arc.

These stress fields and tilts are relevant when studying the propagation of fractures in faults or cavities of the crust of the Earth and the deformations observed in underground cavities.

Appendix 1

Components of the displacement and of the stress tensor around an ellipsoidal cavity in a medium subject to a shear stress p_1 parallel to the x axis:

$$U = \frac{I^2 p_1}{2\mu N_1 h}\left\{ N_1 \cosh 2u + (1+3\sinh^2 u_0)\left[(1+2\sinh^2 u)T - 2\sinh u\right] \right.$$

$$\left. + \frac{\sinh u \cosh^2 u_0}{\cosh^2 u} + a\ \left[-T + \sinh u (T\sinh u - 1)\right]\right\} \sin v \cos v \cos w;$$

$$V = \frac{I^2 p_1}{2\mu N_1 h}\left\{\left[N_1 \sinh u \cosh u - (2-3\cosh^2 u_0)\cosh u (T\sinh u - 1) + \frac{\cosh^2 u_0}{\cosh u}\right]\right.$$

$$\left. \cdot \cos 2v + a\left[(T\sinh u - 1)\cosh u (1+\cos^2 v) + \frac{\sin^2 v}{\cosh u}\right]\right\} \cos w;$$

$$W = \frac{I\, p_1}{2\mu N_1} \cos v \sin w \left\{ \frac{1}{\cosh u}\left[-N_1 \sinh u \cosh u + (2-3\cosh^2 u_0)\right.\right.$$

$$\left.\left. \cdot \cosh u (T\sinh u - 1) - \frac{\cosh^2 u_0}{\cos \mathrm{h}\, u}\right] - 2\alpha (T\sinh u - 1)\right\};$$

$$\sigma_u = \frac{I^2}{h^2}\left\{ p_1 \sinh 2u - \left[A + (1-\alpha)(B+C)\right]\left(T\sinh 2u - 2\cosh u\right)\right.$$

$$+\left[-\frac{2A}{3} - 4B + (1+\alpha)C\right]\frac{1}{\cosh u} + \left(\frac{2A}{3} + 2B\right)\frac{1}{\cosh^3 u}$$

$$\left. + \frac{I^2}{h^2}\left[(-2B+C)\cosh u + \left(\frac{2A}{3} + 2B\right)\frac{1}{\cosh u}\right]\right\}\sin v \cos v \cos w;$$

$$\sigma_v = \frac{I^2}{h^2}\left\{ -p_1 \sinh 2u + \left[A + (1-\alpha)(B+C)\right]\ \left(T\sinh 2u - 2\cosh u\right)\right.$$

$$+\left[\frac{2A}{3} - 2B + (2-\alpha)C\right]\frac{1}{\cosh u} + \frac{I^2}{h^2}\left[(2B-C)\cosh u\right.$$

$$\left.\left. -\left(\frac{2A}{3} + 2B\right)\frac{1}{\cosh u}\right]\right\}\sin v \cos v \cos w;$$

$$\sigma_w = \frac{I^2}{h^2}\left[(-2B+C)\frac{1-\alpha}{coh\, u} - \left(\frac{2A}{3} + 2B\right)\frac{1}{\cosh^3 u}\right]\sin v \cos v \cos w;$$

$$\tau_{uv} = \frac{I^2 \cos w}{h^2}\left\{ p_1 \cosh^2 u + \left[A + (1-a)(B+C)\right]\left(-T\cosh^2 u + \sinh u\right) + (2B-C)\sinh u\right\}$$

$$+\frac{I^2 \cos w \sin^2 v}{h^2}\left\{ -p_1 \cosh 2u + \left[A + (1-a)(B+C)\right]\right.$$

$$\cdot(T\cosh 2u - 2\sinh u) + \left[-\frac{A}{3} + (\alpha - 1)B\right]\frac{\sinh u}{\cosh^2 u}\Bigg\}$$

$$\left. + \sinh u \frac{I^4 \cos w}{h^4}\left[(-2B+C)\cosh^2 u + \frac{2}{3}A + 2B\right];\right.$$

$$\tau_{uw} = \frac{I}{h}\left\{ p_1 \sinh u + \left[A + (1-\alpha)(B+C)\right]\left(-T\sinh u + 1\right) + \left[-\frac{A}{3} + (\alpha - 1)B\right]\frac{1}{\cosh^2 u}\right\}\sin v \sin w;$$

$$\tau_{uw} = \frac{I}{h}\left\{ -p_1 \cosh u + \left[A + (1-\alpha)(B+C)\right] \cdot (T\cosh u - \tanh u) - \left[\frac{2A}{3} + 2B\right]\frac{\sinh u}{\cosh^3 u}\right\}\cos v \sin w;$$

$$A = 3\left(\frac{1}{2} - \cosh^2 u_0\right)p_1/N_1; \quad B = -\frac{1}{2}p_1/N_1; \quad C = p_1/N_1;$$

$$N_1 = \left[\left(3\cosh^2 u_0 - 2 + \frac{\alpha}{2}\right)(-T_0 \cosh^2 u_0 + \sinh u_0) + 2\sinh u_0\right]\left(\cosh^2 u_0\right)^{-1};$$

$$T_0 = \operatorname{arc\,cot}(\sinh u_0).$$

where μ is the rigidity, $\alpha = 2(1 - 1/m)$, and $1/m$ is the Poisson ratio which is assumed here at 0.25. I is assumed as $I = 1/\cosh u_o$ in order to imply ellipsoids with unit semimajor axis along the y axis.

Appendix 2

Components of the displacement and of the stress tensor around an ellipsoidal cavity in a medium subject to a tension or compression p normal to the equator of the cavity and this is subject to a normal tension or compression k:

$$U = \frac{I^2}{2h\mu}\left\{\frac{-P}{4-\alpha}(4-3a)\cosh u \sinh u \sin^2 v - \frac{2p}{4-\alpha}(\alpha - 1)\sinh u \cosh u + \frac{A}{\cosh u} - B\left[6T\cosh u \sinh u - \frac{3\cosh^2 u - 2}{\cosh u} - 3\cosh u\right](3\sin^2 v - 2)\right.$$

$$-C\left[2T\sinh u\cos\mathrm{h}\,u-\frac{\sinh^2 u}{\cosh u}-\cosh u\right]\cos^2 v$$

$$+2\alpha\left[\frac{p}{4-z}\sinh u+C(T\sinh u-1)\right]\cos^2 v\cosh u\Big\};$$

$$V=\frac{I^2}{2hm}\left\{-\frac{p}{4-a}\left[2-a+(4-3z)\sinh^2 u\right]-6B\left[(1+3\sinh^2 u)T-3\sinh u\right]\right.$$

$$\left.+2(1-a)C\left[T\sinh u-1\right]\sinh u-2\alpha\frac{p}{4-\alpha}\sinh^2 u\right\}\sin v\cos v;$$

$$W=0;$$

$$\sigma_u=\frac{I^2}{h^2}\left\{p\cosh^2 u-A\frac{\sinh u}{\cosh^2 u}+B\left[12T\cosh^2 u-12\sinh u-\frac{4\sinh u}{\cosh^2 u}\right]\right.$$

$$\left.+C\left[aT\cosh^2 u+(1-\alpha)\sinh u+\frac{\sinh u}{\cosh^2 u}\right]\right\}+\frac{\sin^2 v}{h^2}I^2\left\{-p\,coh^2 u\right.$$

$$+B\left[-T(18\cosh^2-6)+18\sinh u+6\frac{\sinh u}{\cosh^2 u}\right]+C\left[(2-2\alpha)(T\cosh^2 u\right.$$

$$\left.\left.-\sinh u)+(\alpha-2)T-\frac{\sinh u}{\cosh^2 u}\right]\right\}+I^4\frac{\sinh u}{h^4}\left\{-A-4B-C\sinh^2 u\right\};$$

$$\sigma_v=\frac{I^2}{h^2}\left\{B\left[-6T\cosh^2 u+6\sinh u\right]+C\left[(2-\alpha)T\cosh^2 u+(z-3)\sinh u\right]\right\}+\frac{I^2\sin^2 v}{h^2}$$

$$\cdot\left\{p\sinh^2 u+B\left[(18\cosh^2 u-12)T-18\sinh u\right]+C\left[(-2+2\alpha)\right.\right.$$

$$\left.\left.\cdot T\cosh^2 u-\alpha T+(2-2\alpha)\sinh u\right]\right\}+\frac{I^4\sinh u}{h^4}\left(A+4B+C\sinh^2 u\right);$$

$$\sigma_w = \frac{I^2}{b^2}\left\{A\frac{\sinh u}{\cosh^2 u} + B\left[-6T\cosh^2 u + 6\sinh u + 4\frac{\sinh u}{\cosh^2 u}\right]\right.$$

$$\left. + C\left[(2-\alpha)(T\cosh^2 u - \sinh u) - \frac{\sinh u}{\cosh^2 u}\right]\right\}$$

$$+ \frac{I^2 \sin^2 v}{h^2}\left\{B\left(6T - 6\frac{\sinh u}{\cosh^2 u}\right) + C\left[(\alpha-2)T + \frac{\sinh u}{\cosh^2 u}\right]\right\};$$

$$\tau_{vw} = \tau_{uw} = 0;$$

$$\tau_{uv} = I^2 \frac{\sin v \cos v}{h^2}\left\{-p\sin u\cosh u + B\left[-18T\sinh u\cosh u + 18\cosh u\right.\right.$$

$$\left.\left. - \frac{6}{\cosh u}\right] + C\left[(2-2\alpha)(T\sinh u - 1)\cosh u + \frac{1-\alpha}{\cosh u}\right]\right\} + \frac{\sin v\cos v}{h^4\cosh u}N;$$

$$A = \left\{4\left[(p-k)d^2H + (pd^2-k)E\right] - \left[D(pd^2-k) + (p-k)d^2G\right]\sinh^2 u_O\right\}/J;$$

$$B = \left[(k-p)d^2H + (k-pd^2)E\right]/J;$$

$$C = \left[(pd^2-k)D + (p-k)d^2G\right]/J;$$

$$D = 12d^2 T_0 - 12\sinh u_0; \quad E = \alpha T_0 d^2 + (2-\alpha)\sinh u_0;$$

$$G = (-18d^2 + 6)T_0 + (18 + 6/d^2)\sinh u_0;$$

$$H = T_0\left[(2-2\alpha)d^2 + \alpha - 2\right] + \left(2\alpha - 2 - 1/d^2\right)\sinh u_0;$$

$$J = DH - EG;$$

$$N = I^4\left(A + 4B + C\sinh^2 u\right);$$

$$T = \operatorname{arc\,cot}(\sinh u);$$

where the symbols have the same meaning as in Appendix 1.

References

Caputo M.; 1979: *Two thousand years of geodetic and geophysical observations in the Phlegrean Fields near Naples*. Geophys. J. R. Astr. Soc., **56**, 319-328.

Caputo M.; 1984: *Relaxation and free modes of a self gravitating planet*. Geophys. J. R. Astr. Soc., **77**, 789-808.

Caputo M.; 1990: *The stress and displacement in an anelastic field containing an ellipsoidal cavity*. Atti Accad. Naz. Lincei, Rend. Fisici, **9**, 357-371.

Eshelby J. D.; 1957: *The determination of an anelastic field on an ellipsoidal inclusion and related problems*. Proc. Roy. Soc., Ser. A, **241**, 376-396.

Harrison J. C.; 1976: *Cavity and topographic effects in tilt and strain measurements*. J. Geophys. Res., **81**, 319-328.

Keilis Borok V. I.; 1959: *On estimation of a displacement in an earthquake source and of source dimension*. Annali di Geofisica, **12**, 205-214.

King G. C. P. and Bilham R. G.; 1973: *Tilt measurement in Europe.* Nature, **243**, 74.

Marechal J. C.; 1975: *Some geophysical implications of phase transitions inside the Earth*. PhD thesis, Texas A&M University, pp.126.

Neuber H.; 1937: *Kerbspannungslehere, Grundlagen für genaue Festigkeitsberechnung*. Springer Verlag, Berlin, pp. 185.

Neuber H.; 1958: *Kerbspannungslehere, Grundlagen für genaue Festigkeitsberechnung mit Berucksich tigung von konstructionform und Werkstoff*. Springer Verlag, Berlin, 226 pp.

Palumbo A.; 1978: *Personal communication*.

Sato T. and Harrison J. C.; 1990: *Local effects on tidal and strain measurements at Esashi, Japan*. Geophys. J. Intern., **102**, 513-526.